



# Metals in M33

## Radial gradients and 2D maps

Laura Magrini<sup>1</sup>

Istituto Nazionale di Astrofisica – Osservatorio Astrofisico di Arcetri, Largo E. Fermi, 5,  
I-50125 Firenze, Italy e-mail: laura@arcetri.astro.it

**Abstract.** The metal content of the spiral galaxy M33 is analyzed through spectroscopic observations of its emission-line populations, H II regions and Planetary Nebulae (PNe): their abundance gradients are identical within the errors. The 2D metallicity map is presented, finding an off-center peak, located in the southern arm. A chemical evolution model of M33 described by Magrini et al. (2007a) is updated at the light of recent results on the Schmidt law and the metallicity gradients.

**Key words.** Galaxies: abundances, evolution - Galaxies, individual: M33

### 1. Introduction

M33 (NGC 598) is a spiral galaxy whose closeness (840 kpc, Freedman et al. 1991; optical size  $53' \times 53'$ , Holmberg 1958) and inclination ( $i=53^\circ$ ) allow detailed studies of its stellar populations and ionized nebulae. Planetary Nebulae (PNe) and H II regions represent two very different stages in the lifetime of a galaxy, and their comparison provides insight on the chemical evolution of the host galaxy. PNe are indeed the final ejecta of evolved low- and intermediate-mass stars with mass between 1 and  $8 M_\odot$ , which must have formed between  $3 \times 10^7$  yr and 10 Gyr ago, e.g., Maraston (2005), while H II regions belong to a very young population.

One of the most debated questions about the chemical evolution of galaxies is the metallicity gradient behaviour with time. Chemical evolution models predict different temporal behaviors of the metallicity gradient, depending

on the assumptions one makes on gas inflow and outflow rates, and the star and cloud formation efficiencies. Observations are needed to constrain these assumptions, but so far they have been insufficient, especially for the older populations. The idea behind the observations leading to our work is to study the chemical and physical properties of a large number of PNe and H II regions in M33, using the same set of observations, the same data reduction and analysis techniques, and identical abundance determination methods, to avoid all biases due to the stellar vs. nebular analysis. The aim is to derive abundances of the  $\alpha$ -elements for as many PNe and H II regions as possible, and to study the variation of the metallicity gradient and the average abundances in M33.

In this paper, several aspects of the study of M33 will be described. In Section 2 the observations of a sample of PNe and H II regions with MMT will be presented. These data, together with a large literature data-set, allow us

to recompute the PN and H II region metallicity radial gradients. In Section 3 the spatial distribution of the metallicity will be shown. The off-center of the metallicity maps obtained from H II regions and from PNe will be discussed. In Section 3.2 the chemical evolution model of M33 (Magrini et al. 2007a, hereafter M07) will be revised, including a star formation process, parametrized by a Schmidt law, consistent with the observations. The consequences, in particular the time evolution of the metallicity gradient, will be analyzed. Finally, our conclusions and summary will be given in Section 4.

## 2. The MMT observations

In semester 2007B we observed  $\sim 150$  ionized nebulae in M33 in multi-object spectroscopic mode. We used the Hectospec fiber-fed spectrograph (Fabricant et al. 2005) on the Multi Mirror Telescope (MMT), with a  $270 \text{ mm}^{-1}$  grating at a dispersion of  $1.2 \text{ \AA pixel}^{-1}$ . The instrument deploys 300 fibers over a  $1^\circ$  diameter field of view; the fiber diameter is  $1.5''$  (6 pc using a distance of 840 kpc to M33). We obtained spectra of 102 PNe and 48 HII regions with resulting total spectral coverage from 3600 to 9100  $\text{\AA}$ . The details on the data reduction and analysis are in Magrini et al. (2009, hereafter M09). Most of the PNe observed in M33 belong to its disk, and they are non-Type I, implying a population mainly composed by PNe with old progenitors, i.e.  $M < 3 M_\odot$ , and ages  $> 0.3 \text{ Gyr}$ .

The MMT observations allowed us to obtain a good determination of the O/H gradient (together with Ne/H, S/H, and Ar/H) both from H II regions and PNe. In the case of H II regions, our cumulative sample includes: i) H II regions by Magrini et al. (2007b) which comprises their own determinations and all previous abundance determinations with available  $t_e$ , recomputed uniformly; ii) the sample by Rosolowsky & Simon (2008); iii) the new MMT sample. For PNe, we use the sample of PNe presented by M09. The resulting gradients are the following, for PNe and H II regions respectively,  $12 + \log(\text{O}/\text{H}) =$

$$-0.031(\pm 0.013) R_{\text{GC}} + 8.44(\pm 0.06), \quad (1)$$

$$-0.032(\pm 0.009) R_{\text{GC}} + 8.42(\pm 0.04), \quad (2)$$

where  $R_{\text{GC}}$  is the galactocentric distance in kpc. The two gradient are identical within the errors, both in their slopes and central values.

## 3. The metallicity in M33 and its evolution

The large amount of chemical abundance data from H II regions and PNe collected to date in M33 allow us to reconstruct its metallicity map. In this section, both the 2D and the radial distribution are analyzed taking advantages also of all previous abundance determinations with measured  $t_e$  and of our new results.

### 3.1. The 2D distribution of metals

The usual way to study the metallicity distribution in disk galaxies is to average it azimuthally, assuming that: i) the centre of the galaxy coincides with the peak of the metallicity distribution; ii) at a given radius, the metallicity is the same in each side of the galaxy. The large number of metallicity measurements in M33, both from H II regions and from PNe, allow us to reconstruct not only their radial gradient, but also their spatial distribution projected onto the disk. In Figure 1, the two-dimensional metallicity distributions for M33 from H II regions and from PNe are shown. The highest metallicity H II regions and PNe are not located at the center of the galaxy, but rather lie at a radius of 1-2 kpc, in the southern arm. Simon & Rosolowsky (2008) noticed this behavior for H II regions and suggested as explanation that the material enriched by the most recent generation of star formation in the arm has not yet been azimuthally mixed through the galaxy. Whilst it might be true for H II regions, it cannot be the reason for the off-center metallicity distribution of PNe since they belong to an older population. Colin & Athanassoula (1981) noticed several evidences of asymmetries in the inner regions of M33, such as the distribution of HI atomic gas, of H II regions, of high luminosity stars. They proposed a kine-

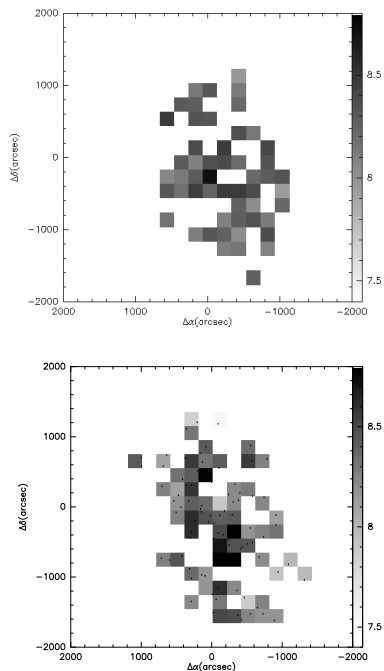


**Fig. 1.** The metallicity maps: PNe (top) and H II regions (bottom). The  $12 + \log(\text{O}/\text{H})$  scale is shown on the y axis. The centre of M33 corresponds to the 0,0 position.

mathematical model with a displaced bulge having a retrograde motion around the center. Also detailed analysis of the innermost regions of M33 by Corbelli & Walterbos (2007) found possible asymmetries in the stellar and gas velocity pattern which might be related to the displacement of a small bulge. The off-center metallicity distribution might thus be related to the lack of a dominant gravitational source in the center of this galaxy with a consequent motion at different epochs of the peak of the highest star formation region around the M33 visual center.

### 3.2. The time-evolution of the abundance gradient

M07 built a chemical evolution model of M33, called *accretion* model, able to reproduce its main features, including the radial trends at present-time of molecular gas, atomic gas,

stars, SFR, and the time evolution of the metallicity gradient using the available constraints at that time. In that model, the disk of M33 was formed by continuous accretion of primordial gas from the intergalactic medium. However, new observations have been made recently available, rendering necessary a revision of the model. In particular, the global slope of the radial O/H gradient has been confirmed much shallower than retained in the past (cf. Rosolowsky & Simon 2008) and its evolution much slower (cf. M09).

The general assumption of multiphase chemical evolution models, such as the M33 one (M07), is to describe the formation and disruption of diffuse gas, clouds, and stars, by means of physical processes, e.g., Ferrini et al. (1992). In particular, the SF is represented with two processes: the interaction of molecular clouds with the radiation field of massive stars and the collisions between two molecular clouds. The dominant process is due to cloud collisions. In this kind of model the relationship between the star formation rate (SFR) and the surface density of gas (molecular or total) is, thus, a by-product of the model, and cannot be assumed 'a priori'.

However, the law relating the surface densities of SF and cold gas is one of the most fundamental laws describing the galaxy behaviour. Virtually the entire range of global star formation rates in galaxies can be reproduced by a Schmidt power law relation. In the particular case of M33, the relation between the SFR, measured from the FUV emission, and molecular gas has a well-defined slope (Verley et al., in prep.) corresponding to

$$\Sigma_{SFR} = A \Sigma_{molgas}^{1.2}. \quad (1)$$

A pure cloud-cloud collision process for the star formation is not able to reproduce it. For this reason, we have taken into account other parameterizations of the SF process. In particular, a process which is dominated by cloud collisions close to the center, while in the intermediate and peripheral regions is proportional to the fraction of clouds with a 1.5 exponent, is able to reproduce the observations. It reproduces the higher cloud surface density in the inner regions, rendering the conversion

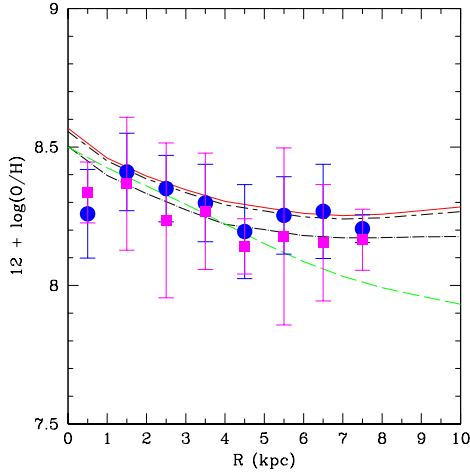


**Fig. 2.** The time-evolution of the O/H radial gradient. Filled symbols (blue circles and magenta squares) are the oxygen abundances of H II regions and PNe, respectively, averaged in bins 1 kpc wide. Model with the Schmidt law: present time (red continuous line), 1 Gyr ago (long-short dashed line), 5 Gyr ago (dot-dashed line). Model with the cloud-cloud collision process (M07): present time (green dashed line).

into star less effective, while in the outer regions it takes into account a more efficacious SF. The resulting Schmidt law would have an average exponent all over the radial range (or the molecular gas surface density range) of 1.1, thus consistent with the observations.

In addition, the introduction of the Schmidt law allowed us to better reproduce the O/H gradient and its evolution (see Figure 2): a gradient almost flat both at present-time both at the epoch of the formation of the PNe progenitors, with a little evolution of its absolute value and slope. Note from Figure 2 the steeper gradient predicted by the previous model, where the SF process was dominated by cloud-cloud collision all over the radial range.

#### 4. Summary and conclusions

The chemical evolution of M33 is studied by means of new spectroscopic observations of PNe and H II regions. Their 2D metallicity maps have been found both off-centered, with

a peak in the southern arm, at 1-2 kpc from the center. This might be related to the absence of a dominant gravitational source in the center. The slow evolution of the metallicity gradient from the present time to the birth of the PNe progenitors is explained with an *accretion* model where the SF process is driven by the Schmidt law.

*Acknowledgements.* I warmly thank Edvige Corbelli, Daniele Galli, Letizia Stanghellini, and Eva Villaver for their collaboration in this work.

#### References

- Colin J., Athanassoula E., 1981, *A&A*, 97, 63  
 Corbelli E., Walterbos R. A. M., 2007, *ApJ*, 669, 315  
 Fabricant, D., et al. 2005, *PASP*, 117, 1411  
 Ferrini, F., Matteucci, F., Pardi, C., Penco, U. 1992, *ApJ*, 387, 138  
 Freedman, W. L., Wilson, C. D., Madore, B. F. 1991, *ApJ*, 372, 455  
 Holmberg, E., 1958, *Lund Medd. Astron. Obs. Ser. II*, 136, 1  
 Magrini L., Corbelli E., Galli D., 2007a, *A&A*, 470, 843 (M07)  
 Magrini, L. et al. 2007b, *A&A*, 470, 865  
 Magrini L., Stanghellini L., Villaver E., 2009, *ApJ*, 696, 729 (M09)  
 Maraston, C. 2005, *MNRAS*, 362, 799  
 Rosolowsky, E., Simon, J. D., 2008, *ApJ*, 675, 1213  
 Simon J. D., Rosolowsky E., 2008, *ASPC*, 396, 23